International Journal of Power Electronics and Drive System (IJPEDS)
Vol. 3, No. 4, December 2013, pp. 351~364
ISSN: 2088-8694

Hybrid Fuzzy Sliding Mode Control of a DFIG Integrated into the Network

Belabbas Belkacem[1], Tayeb Allaoui[2], Mohamed Tadjine[3], Ahmed Safa[4]
[1,2]Laboratoire de Génie Energitique et Génie Informatique LGEGI, Université Ibn Khaldoun de Tiaret, Algérie
[3]Laboratoire de Commandes des Processus, Ecole Nationale Polytechnique Alger, Algérie
[4]Laboratoire de génie électrique et de Plasma LGEP, Tiaret, Algérie

Article Info

Article history:

Received Aug 8, 2013
Revised Sep 15, 2013
Accepted Oct 6, 2013

Keyword:

DFIG
FSMC
SMC
three-level converter structure NPC
Vector control
Wind System

ABSTRACT

This paper presents the study of a variable speed wind energy conversion system using a Doubly Fed Induction Generator (DFIG) based on a Fuzzy sliding mode control (FSMC) applied to achieve control of active and reactive powers exchanged between the stator of the DFIG and the grid to ensure a Maximum Power Point Tracking (MPPT) of a wind energy conversion system. However the principal drawback of the sliding mode, is the chattering effect which characterized by torque ripple, this phenomena is undesirable and harmful for the machines, it generates noises and additional forces of torsion on the machine shaft. In order to reduce the chattering effect, the Sign function of sliding mode controller's discontinuous part is replaced by a fuzzy logic; we will have the fuzzy sliding mode controller (FSMC). The FSMC makes it possible to combine the performances of the two types of controllers (SMC and FLC) and eliminates the chattering effect. The proposed control algorithm is applied to a DFIG where the stator is directly connected to the grid and the rotor is connected to a three-level converter structure NPC to suppress low level harmonics, higher frequencies will be filtered out by the machine. Second goal of this paper is to extract a maximum of power; the rotor side converter is controlled by using a stator flux-oriented strategy. The decoupling created by the control between active and reactive stator power allows keeping the power factor close to unity. Simulation results show that the wind turbine can operate at its optimum energy for a wide range of wind speed. Both simulation and validation results show effectiveness of the proposed control strategy is in terms of power regulation. Moreover, the fuzzy sliding mode approach is arranged so as to reduce the chattering produced in the generated power that could lead to increased mechanical stress because of strong torque variations.

Corresponding Author:

Belabbas Belkacem,
Laboratory of Energy Engineering and Computer Engineering
University Ibn Khaldun Tiqret, Algeria
Email: belabbas_1986@yahoo.fr

1. INTRODUCTION

Wind energy is one of the fastest growing renewable energy in the world. The generation of wind energy is clean, non-polluting, it produces no harmful wast to the environment. Conventional techniques were used to adjust the wind, but assuming the wind operation in balanced conditions. Advances in technology of wind led to the design of a more powerful drive to improve their behavior and make it more robust and reliable. One of the current areas of research is the generation of electrical energy by means of double-fed asynchronous machine, using driving means such as wind power incorporated into a wind energy system. Diagram of a conversion of wind energy is shown as Figure 1.

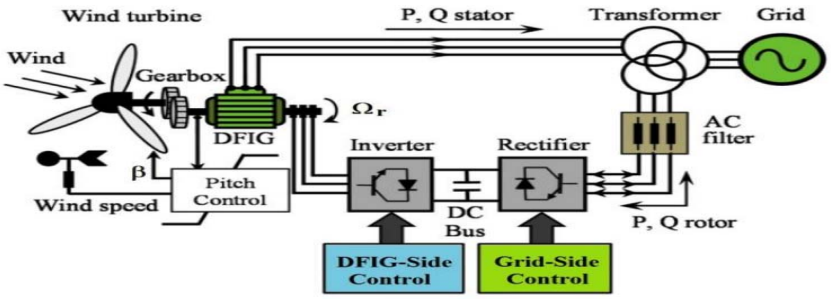

Figure1. Diagram of a Conversion of Wind Energy.

Recently, the doubly fed induction generator (DFIG) is becoming the main configuration of wind power generation because of its unique advantages. Vector control technology is used to control the generator, and the rotor of DFIG is connected to an AC excitation of which the frequency, phase, and magnitude can be adjusted [1].

Therefore, constant operating frequency can be achieved at variable wind speeds. A doubly fed induction generator is most commonly used in wind power generation. It is a wound rotor induction machine with slip rings attached at the rotor and fed by power converter. With DFIG, generation can be accomplished in variable speed ranging from sub-synchronous speed to super-synchronous speed.

The variable speed constant frequency wind power generation is mainly based on the research of optimal power-speed curve, namely the most mechanical power of turbine can be achieved by regulating the speed of generator, where the wind speed may be detected or not.

Through studying the characteristics of wind turbine, the paper proposed the maximum power point tracking (MPPT) control method. Firstly, according to the DFIG character, the paper adopts the vector transformation control method of stator oriented magnetic field to realize the decoupling control for the active power and reactive power using sliding mode control (SMC) and fuzzy sliding mode control (FSMC).

Sliding mode theory, stemmed from the variable structure control family, has been used for the induction motor drive for a long time. It has for long been known for its capabilities in accounting for modeling imprecision and bounded disturbances. It achieves robust control by adding a discontinuous control signal across the sliding surface, satisfying the sliding condition. Nevertheless, this type of control has an essential drawback, which is the chattering phenomenon caused from the discontinuous control action.

The idea is this combined control (SMC) also advanced by a controller is called Fuzzy (FLC) to reduce these phenomena chattering. Simulation results of this FSMC show good performance and considerable reduction of the chattering phenomenon.

2. RESEARCH METHOD

2.1. Modeling of wind turbine

2.1.1. Modeling of wind turbine

Mechanical power available on the shaft of a wind turbine is expressed by [1] [4]:

$$P_{aero} = \frac{1}{2}.C_p(\lambda,\beta).\rho.\pi.R^2.V^3 \quad (1)$$

$$\lambda = \frac{R.\Omega_{mec}}{G.V} \quad (2)$$

The aerodynamic torque is directly determined by [1]:

$$C_{aero} = \frac{P_{aero}}{\Omega_{Turbine}} = C_P.\frac{\rho.S.V_1^3}{2.\Omega_{Turbine}} \quad (3)$$

The multiplier is mathematically modeled by the following equations:

$$C_g = \frac{C_{aero}}{G} \quad (4)$$

$$\Omega_{turbine} = \frac{\Omega_{mec}}{G} \tag{5}$$

The power factor $C_P(\lambda,\beta)$ represents the aerodynamic efficiency of the wind turbine. The wind turbine is a complex model, however simple mathematical models are often used aerodynamic system. The expression of power coefficient that we will use in our study is given by [1]:

$$Cp(\lambda,\beta) = 0.5176.\left(116.\frac{1}{\lambda i} - 0.4.\beta - 5\right).\exp\left(\frac{-21}{\lambda i}\right) + 0.0068.\lambda i \tag{6}$$

$$\frac{1}{\lambda_i} = \frac{1}{\lambda + 0.08.\beta} - \frac{0.035}{1+\beta^3} \tag{7}$$

The fundamental equation of dynamics to determine the evolution of the mechanical speed from the total mechanical torque (C_{mec}) applied to the rotor:

$$\begin{aligned} J.\frac{d\Omega_{mec}}{dt} &= C_{mec} \\ C_{mec} &= C_g - C_{em} - C_{vis} \\ C_{vis} &= f.\Omega_{mec} \\ J &= \frac{J_{turbine}}{G^2} + J_g \\ f &= \frac{f_{turbine}}{G^2} + f_g \end{aligned} \tag{8}$$

In this section, we present a different strategy to control the electromagnetic torque to adjust the mechanical speed to maximize the electric power generated. This principle is known as the terminology (MPPT).

We are interested in controlling the electromagnetic torque servo mechanical speed using a conventional PI controller. For this study, we assume that the electrical machine and its drive are ideal and therefore, regardless of the power generated, the electromagnetic torque is developed at all times equal to its reference value. The maximum power extraction techniques include determining the speed of the turbine, which provides maximum power generated [8].

$$\frac{d\Omega_{mec}}{dt} = \frac{1}{J}.(C_g - C_{em} - f.\Omega_{mec}) \tag{9}$$

$$\begin{aligned} C_{emref} &= PI.(\Omega_{ref} - \Omega_{mec}) \\ \Omega_{ref} &= G.\Omega_{turbine\ ref} \\ \Omega_{turbine\ ref} &= \frac{\lambda.C_{p\max}.V}{R} \end{aligned} \tag{10}$$

2.1.2. Model of DFIG

Applying the Park transformation to electrical equations DFIG [1] in the referencial linked to the rotating field allows us to achieve the following electrical system of equations:

The stator and rotor equation in the referencial synchronous are given by:

$$\begin{cases} V_{sd} = R_s i_{sd} + \frac{d\Phi_{sd}}{dt} - \omega_s \Phi_{sq} \\ V_{sq} = R_s i_{sq} + \frac{d\Phi_{sq}}{dt} + \omega_s \Phi_{sd} \\ V_{rd} = R_r i_{rd} + \frac{d\Phi_{rd}}{dt} - \omega_r \Phi_{rq} \\ V_{rq} = R_r i_{rq} + \frac{d\Phi_{rq}}{dt} + \omega_r \Phi_{rd} \end{cases} \tag{11}$$

$$\begin{cases} \Phi_{sd} = L_s i_{sd} + M_{sr} i_{rd} \\ \Phi_{sq} = L_s i_{sq} + M_{sr} i_{rq} \\ \Phi_{rd} = L_r i_{rd} + M_{sr} i_{sd} \\ \Phi_{rq} = L_r i_{rq} + M_{sr} i_{sq} \end{cases} \quad (12)$$

$$C_{em} = P \frac{M_{sr}}{L_s} \left(\Phi_{sq} i_{rd} - \Phi_{sd} i_{rq} \right) \quad (13)$$

2.1.3. Power control

To easily control the production of electricity from wind, we will achieve an independent control of active and reactive power by the stator flux orientation. The idea is to align along the axis of the rotating frame [2] stator flux. We therefore: $\Phi_{sq} = 0$ and consequently $\Phi_{sd} = \Phi_s$.

This choice is not random but is justified by the fact that the machine is often coupled with a powerful network voltage and constant frequency, which leads to a finding stator flux of the machine. Neglecting the resistance of the stator windings, often accepted hypothesis for high power machines: The systems of equations (11) and (12) can be simplified as follows:

$$\begin{cases} V_{sd} = 0 \\ V_{sq} = V_s = \omega_s \Phi_s \\ V_{rd} = R_r i_{rd} + \dfrac{d\Phi_{rd}}{dt} - \omega_r \Phi_{rq} \\ V_{rq} = R_r i_{rq} + \dfrac{d\Phi_{rq}}{dt} + \omega_r \Phi_{rd} \end{cases} \quad (14)$$

$$\begin{cases} \Phi_s = L_s i_{sd} + M_{sr} i_{rd} \\ 0 = L_s i_{sq} + M_{sr} i_{rq} \\ \Phi_{rd} = L_r i_{rd} + M_{sr} i_{sd} \\ \Phi_{rq} = L_r i_{rq} + M_{sr} i_{sq} \end{cases} \quad (15)$$

$$Cem = -P \frac{Msr}{Ls} \Phi s \; irq \quad (16)$$

The stator active and reactive power in the orthogonal coordinate system can be written:

$$\begin{cases} P = v_{sd} i_{sd} + v_{sq} i_{sq} \\ Q = v_{sq} i_{sd} - v_{sd} i_{sq} \end{cases} \quad (17)$$

Under the assumption of a stator flux oriented, this system of equations can be simplified as:

$$\begin{cases} P = v_s i_{sq} \\ Q = v_s i_{sd} \end{cases} \quad (18)$$

From the expressions of the stator flux, we can write:

$$\begin{cases} i_{sd} = \dfrac{V_s}{\omega_s L_s} - \dfrac{Msr}{L_s}.i_{rd} \\ i_{sq} = -\dfrac{Msr}{L_s}.i_{rq} \end{cases} \quad (19)$$

$$\begin{cases} P = -\dfrac{V_s M_{sr}}{L_s} i_{rq} \\ Q = -\dfrac{V_s M_{sr}}{L_s} i_{rd} + \dfrac{V_s^2}{L_s \omega_s} \end{cases} \quad (20)$$

$$\begin{cases} \Phi_{rd} = \left(L_r - \dfrac{M_{sr}^2}{L_s} \right) i_{rd} + \dfrac{M_{sr} V_s}{\omega_s L_s} \\ \Phi_{rq} = \left(L_r - \dfrac{M_{sr}^2}{L_s} \right) i_{rq} \end{cases} \quad (21)$$

By introducing these expressions in the equations of the rotor voltages are found:

$$\begin{cases} V_{rd} = R_r i_{rd} + \left(L_r - \dfrac{M_{sr}^2}{L_s} \right) \dfrac{di_{rd}}{dt} - g\omega_s \left(L_r - \dfrac{M_{sr}^2}{L_s} \right) i_{rq} \\ V_{rq} = R_r i_{rq} + \left(L_r - \dfrac{M_{sr}^2}{L_s} \right) \dfrac{di_{rq}}{dt} + g\omega_s \left(L_r - \dfrac{M_{sr}^2}{L_s} \right) i_{rd} + g \dfrac{M_{sr} V_s}{L_s} \end{cases} \quad (22)$$

2.2. Indirect controls with power LOOP

It is based on the equations governing the operation of the machine defined in the preceding paragraph, while keeping the same assumptions.

By combining the different flow equations, the rotor voltages, currents and powers, we can write the equations of the rotor voltage depending on the power. Thus power from the stator as a function of the rotor currents and voltages of the rotor in terms of the rotor current function [1]:

From the control unit we can develop a structure ensures good stability of the network, so we have a control unit consists of two subsystems. The first calculates the reference currents from the references (active and reactive powers), the second calculates the reference voltage from the rotor currents calculated by the first. In this spirit, we have used SMC to the inner loop (current loop) and classic PI outer loop to controlling powers. It then sets the control system given by the Figure 2.

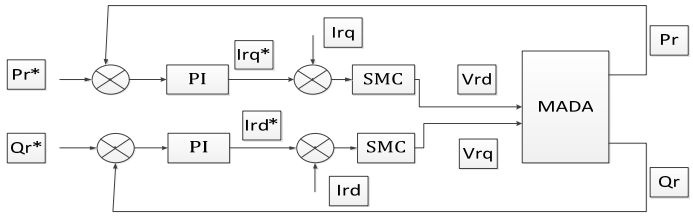

Figure 2. Block diagram of indirect control with loop power controlled by SMC**.**

2.3. Devoloping of the hybrid control

2.3.1. Indirect control of the dfig with loop power

The basic idea of the SMC is primarily attracting states of the system in a suitably selected, and then designs a control law that will always keep the system in this region (Ardjoun et al, 2011) region. In summary SMC is divided into three parts: [1] [2] [3] [5] [6].

2.3.1.1. Choice of switching surface

For a non-linear system shown in the following form:

$$\begin{aligned} &\dot{X} = f(X,t) + g(X,t) \quad u(X,t); \\ &X \in R^n, u \in R. \end{aligned} \tag{23}$$

There f (X, t), g(X, t) are two continuous and uncertain nonlinear functions, assumed bounded. It takes the form of general equation proposed by JJSlotine to determine the sliding surface given by (Slotine and al, 1998):

$$S(X) = \left(\frac{d}{dt} + \lambda \right)^{n-1} .e \quad et \quad e = X^d - X \tag{24}$$

With, e: error on the controlled variable, λ: positive coefficient, n: order system, X^d: desired size, X: state variable of the controlled variable.

2.3.1.2. Convergence condition

The convergence condition is defined by the Lyapunov equation (Lopez et al, 2006), it makes the area attractive and invariant $S(X).\dot{S}(X) \le 0$.

2.3.1.3. Control calculation

The control algorithm is defined by the relation $u = u^{eq} + u^n \; et \; u^n = u^{\max}.sign(S(X))$

With: u: control variable, u^{eq}: size equivalent command, u^n: term control switch, sign(S(X)): sign function.

2.3.2. Control of rotor current next axis "D"

To control the rotor current is taken n = 1, the expression of the current control surface along the axis "d" of the marker to form Park $S(I_{rd}) = (I_{rd}^* - I_{rd})$

Deriving the surface with the replacement of the current expression I_{rd}, obtained:

$$\dot{S}(I_{rd}) = (\dot{I}^*_{rd} - \frac{1}{\sigma.L_r}(V_{rd} - R_r.I_{rd}) \tag{25}$$

The control voltage V_{rd} is defined by: $V_{rd} = V_{rd}^{eq} + V_{rd}^n$ During the sliding mode and steady state was: $\dot{S}(I_{rd} = 0); S(I_{rd} = 0); V_{rd}^n = 0;$ or of pulling: $V_{rd}^{eq} = \sigma.L_r.\dot{I}^*_{rd} + R_r.I_{rd}$ During the convergence mode, the condition $S(X).\dot{S}(X) \le 0$ should be checked with: $V_{rd}^n = K.V_{rd}.sign(S(I_{rd}))\; et \; K.V_{rd}$ positive gain.

2.3.3. Control of rotor current next axis "Q"

To control the rotor current is taken n = 1, the expression of the current control surface along the axis "q" of the marker to form Park $S(I_{rq}) = (I_{rq}^* - I_{rq})$

Deriving the surface with the replacement of the current expression I_{rq}, on gets:

$$\dot{S}(I_{rq}) = (\dot{I}^{*}_{rq} - \frac{1}{\sigma.L_r}(V_{rq} - R_r.I_{rq}) \quad (26)$$

The control voltage V_{rq} is defined by: $V_{rq} = V_{rq}^{eq} + V_{rq}^{n}$ During the sliding mode and steady state was: $\dot{S}(I_{rq} = 0); S(I_{rq} = 0); V_{rq}^{n} = 0;$ or of pulling: $V_{rq}^{eq} = \sigma.L_r.\dot{I}^{*}_{rq} + R_r.I_{rq}$ During the convergence mode, the condition $S(X).\dot{S}(X) \le 0$ should be checked with: $V_{rq}^{n} = K.V_{rq}.sign(S(I_{rq}))$ *et* $K.V_{rq}$ positive gain.

2.4. Fuzzy sliding mode control of internal loop DFIG

The disadvantage of the SMC is that the term switching control where we have lot of ripples. To reduce it, we replace it by a fuzzy structure (Wong et al, 2001). FSMC, which is designed to control the rotor current, is shown in Figure 3 [9] [10] [11].

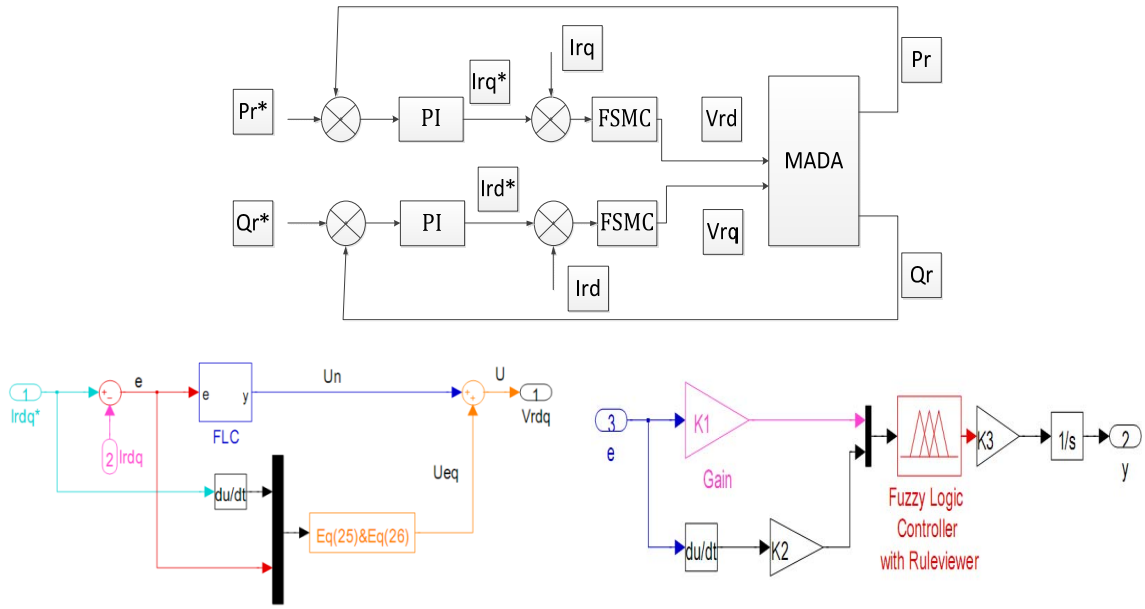

Figure3. Block diagram of indirect control with loop controlled power FSMC.

The fuzzy logic control is expanding. Indeed, this method provides a very effective law often set without doing extensive modeling. As opposed to a standard regulator or a regulator of state-reaction against the controller fuzzy logic does not address a well-defined mathematical relationship, but uses inferences with multiple rules, based on linguistic variables. By inference with several rules, it is possible to take account of experience gained by the operators of a technical process.

Three linguistic variables input-output are shown in Figure 4. The fuzzy rules can be written as shown in Table 1. For this purpose, it is used a system of Mamdani-type fuzzy logic. The membership function is resulted from the aggregation of using the operator max. The Defuzzification of the output control is accomplished using the method of center of gravity.

2.5. Modeling and control of the three levels structure NPC VSI

2.5.1. The three-level NPC VSI structure

The three phases three-level NPC VSI is constituted by three arms and two DC voltage sources. Every arm has four bi-directional switches in series and two diodes (Figure 5) [3].

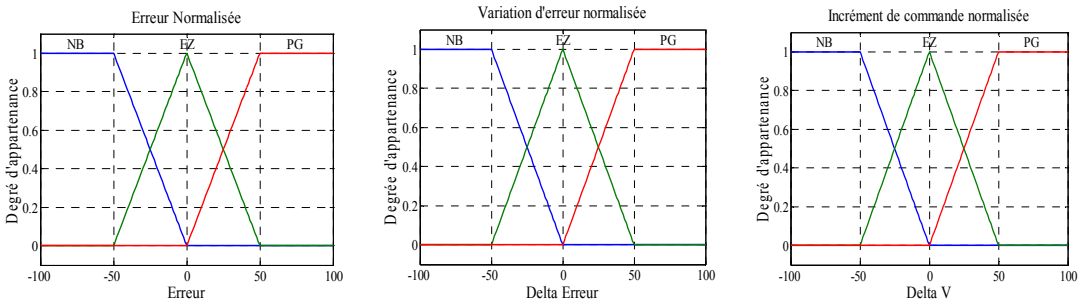

Figure4. Membership functions of the different linguistic variables.

Table1. Ruleset for RFL.

ΔE_X \ E_X	NP	EZ	PG
NP	NP	NP	EZ
EZ	NP	EZ	PG
PG	EZ	PG	PG

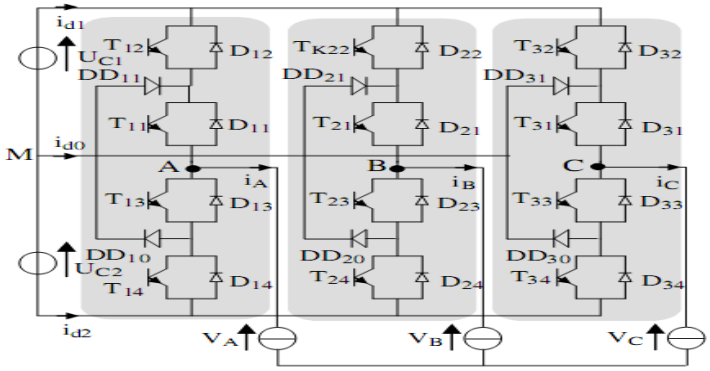

Figure5. The three-level NPC inverter.

2.5.2. Knowledge model

The switch connection function F_{ks} indicates the opened or closed state of the switch T_{ks} .

We define too a half arm connection function F_{km}^{b} with:

K: Arm number.

$$m = \begin{cases} 1 \ \textit{for the lower half arm} \\ 0 \ \textit{for the upper half arm} \end{cases}$$

For an arm k of the three-phase three-level NPC VSI, several complementary laws controls are possible. The control law which lets an optimal control of this inverter is [3]:

$$\begin{cases} B_{k1} = \overline{B}_{k4}. \\ B_{k2} = \overline{B}_{k3}. \end{cases} \quad (27)$$

Where B_{ks} represents the gate control of the switch T_{ks} . We define the half arm connection function F_{i1}^{b} and F_{i0}^{b} associated respectively to the upper and lower half arms.

Where i is arm number $i \in \{1,2,3\}$

$$\begin{cases} F_{11} = 1 - F_{14} \\ F_{12} = 1 - F_{13} \end{cases} \quad \begin{cases} F_{21} = 1 - F_{24} \\ F_{22} = 1 - F_{23} \end{cases} \quad \begin{cases} F_{31} = 1 - F_{34} \\ F_{32} = 1 - F_{33} \end{cases} \tag{28}$$

The output voltages of the inverter relatively to the middle point M are defined as follows:

$$\begin{bmatrix} V_{AM} \\ V_{BM} \\ V_{CM} \end{bmatrix} = \begin{bmatrix} F_{11}^b \\ F_{21}^b \\ F_{31}^b \end{bmatrix} . U_{c1} - \begin{bmatrix} F_{10}^b \\ F_{20}^b \\ F_{30}^b \end{bmatrix} . U_{c2} \tag{29}$$

The system (29) shows that the three-level NPC VSI can be considered as two two-level voltage source inverters in series. The input currents of the inverter are given as follow:

$$\begin{cases} i_{d1} = F_{11}^b . i_1 + F_{21}^b . i_2 + F_{31}^b . i_3 \\ i_{d2} = F_{10}^b . i_1 + F_{20}^b . i_2 + F_{30}^b . i_3 \end{cases} \tag{30}$$

The current i_{d0} is defined by the following relation:

$$i_{d0} = F_{11} . F_{13} . i_1 + F_{21} . F_{23} . i_2 + F_{31} . F_{33} . i_3 \tag{31}$$

2.5.3. PWM strategy of the three-level NPC VSI

The inverter is controlled by the space vector modulation strategy which uses two bipolar carriers. This strategy is characterised by two parameters:
Modulation index m defined as ratio between the carrier frequency fp and the reference voltage frequency:

$$m = \frac{f_p}{f} \tag{32}$$

Modulation rate r is the ratio between the magnitudes Vm of the reference voltageand three times of the carriers magnitude Upm:

$$r = \frac{V_r}{V_p} \leq 1 \tag{33}$$

2.6. Cascade (rectifier, filter and inverter) with DFIG

In this part of the chapter, the dynamic behavior of the wind turbine based on doubly fed machine (DFIG) connected to the network is studied. The stator of the DFIG is directly connected to the network, against the rotor is connected to it via a cascade (rectifier, filter and inverter). This changer allows indirect frequency from a fixed network frequency and amplitude has a system output voltage frequency and variable amplitude. The general structure of this cascade is shown in Figure 6. The rectifier and inverter is controlled by the two sinusoidal carrier strategy triangular sawtooth.

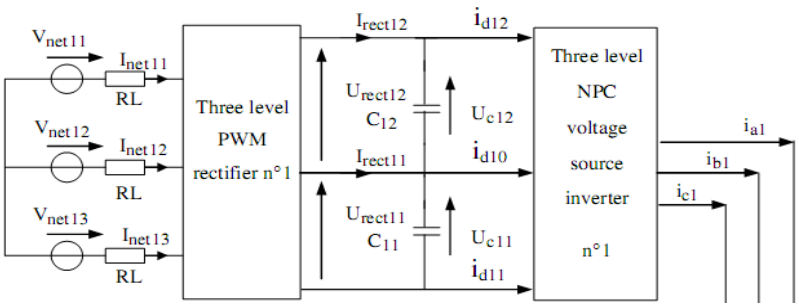

Figure6. Cascade of a turbine, a rectifier - inverter voltage three-phase three-level feeding the DFIG.

2.6.1. Modelling of the intermediate filter

The model of the intermediate filter is defined by the following system:

$$\begin{cases} U_{C1} = \dfrac{1}{C_1}\int (I_{rect1} - I_{d1})dt \\ U_{C2} = \dfrac{1}{C_2}\int (I_{rect2} - I_{d2})dt \end{cases} \quad \begin{cases} C_1.\dfrac{dU_{C1}}{dt} = I_{rect1} - I_{d1} \\ C_2.\dfrac{dU_{C2}}{dt} = I_{rect2} - I_{d2} \end{cases} \tag{34}$$

2.7. The half clamping bridge

To improve the input voltages of the three-level NPC inverter, we propose to use a half clamping bridge, constituted by a transistor and a resistor [3]. The transistors are controlled to maintain equal the different input DC voltages of the inverter (Figure 7).

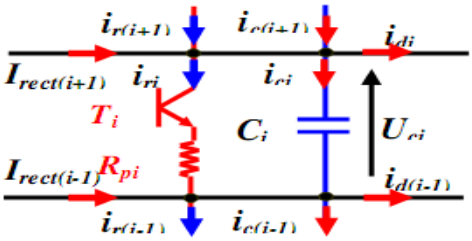

Figure7. Structure Bridge clamping with intermediate filter.

2.7.1. Modelling of the intermediate filter

Figure 8 shows the structure of the intermediate filter of the studied cascade.

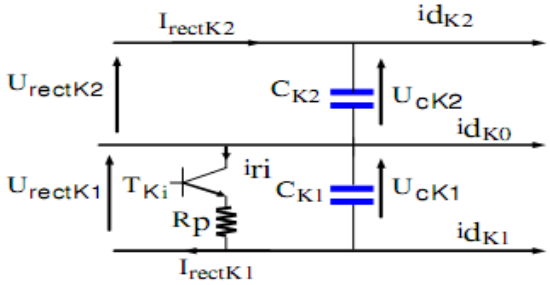

Figure 8. Structure of the intermediate filter of the of the half clamping bridge cascade.

The model of the half clamping bridge-filter set is defined by the following equation:

$$\begin{cases} U_{C1} = \dfrac{1}{C_1}\int (I_{rect1} - I_{r1} - I_{d1})dt \\ U_{C2} = \dfrac{1}{C_2}\int (-I_{rect2} - I_{r2} + I_{d2})dt \end{cases} \tag{35}$$

$$\mathrm{I_{ri}} = \mathrm{T_i}.\frac{\mathrm{U_{Ci}}}{\mathrm{R_{Pi}}} \qquad \text{Avec} \quad \mathrm{i} = \{1, 2\} \tag{36}$$

The control algorithm of the resistive clamping circuits can be summarized as follows:

$$\begin{cases} (U_{Ci} - U_{ref}) = \varepsilon_i \\ if\ \ \varepsilon_i \succ 0\ Then\ T_i = 1 \Rightarrow I_{ri} = T_i.\dfrac{U_{Ci}}{R_{Pi}} \\ if\ \ NO\ T_i = 0 \Rightarrow I_{ri} = 0 \end{cases} \tag{37}$$

2.7.2. Voltage loop model

The modelling of this loop is based on principle of instantaneous power conservation with no loss hypothesis. This boucle imposes efficacy network reference current. The input power is calculated as:

$$P_e = \sum_{K=1}^{3}\left(V_{netK}.i_{netK} - R_{net}.i_{netK}^2 - \frac{L_{net}}{2}\frac{di_{netK}^2}{dt} \right) \quad (38)$$

The output power is calculated as:

$$P_e = U_{C1}.(i_{C1} + i_{load1}) + U_{C2}.(i_{C2} + i_{load2}) = U_{rect1}.I_{rect1} - U_{rect2}.I_{rect2} \quad (39)$$

It is assumed that the following: $U_{C1} = U_{C2} = U_C$ *and* $C_1 = C_2 = C$.

Define variables. i_C, i_{laod} *and* U_C

$$\begin{cases} i_C = \dfrac{i_{C1} + i_{C2}}{2} \\ i_{Ch} = \dfrac{i_{d1inv} - i_{d2inv}}{2} \\ U_C = U_{Cmoy} = \dfrac{U_{C1} + U_{C2}}{2} \\ i_{rec} = i_C + i_{laod} \end{cases} \quad (40)$$

Using the principle of conservation of power and neglecting the Joule losses in the resistance Rnetw, we can write:

$$\sum_{K=1}^{3}(V_{netwK}.i_{netwK}) = \sum_{K=1}^{3}\frac{L_{netwK}}{2}\frac{di_{netwK}^2}{dt} + 2.U_C.(i_C + i_{Laod}) \quad (41)$$

Assuming the sinusoidal line currents in phase with their corresponding voltages, then we can write:

$$3.V_{eff}.I_{eff} = 2.U_C.(i_C + i_{laod}) \quad (42)$$

Where E_{eff} is the rms value of grid voltages and Ie is the rms value of grid currents. Uc is the constant value of the DC capacitor voltage and Irect is the DC current. A IP regulator is used to regulate the DC voltage. The general principle feedback of three-level rectifier is shown on Figure 9.

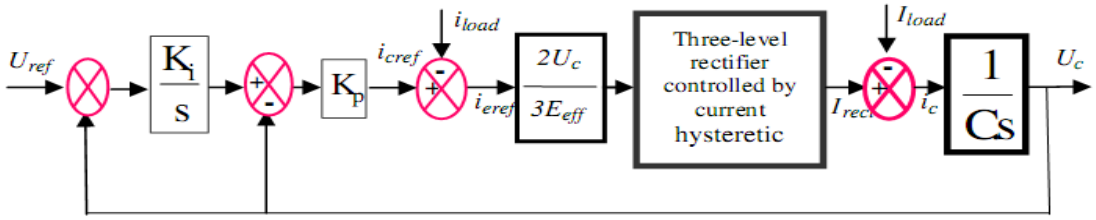

Figure 9. Enslavement algorithm of output voltage of three-level rectifier.

3. RESULTS AND ANALYSIS

In this section, we present the work on the modeling of a chain of wind conversion based on an asynchronous machine is comprised of dual power controlled by the technique of PWM rectifier and a DC bus, all connected to the network via a PWM inverter and a filter. Modeling the overall wind conversion chain and the associated control device are developed in the form of an equivalent continuous model which takes into account the relevant components of the currents and voltages at the machine, and the DC bus network.

We applied a control algorithm on the voltages (Uc1, Uc2) with the aim of stabilizing the past to balance the midpoint M.

The strategy of indirect control based controllers SMC and FSMC rotor currents of DFIG were implemented in MATLAB environment to perform tests of control.

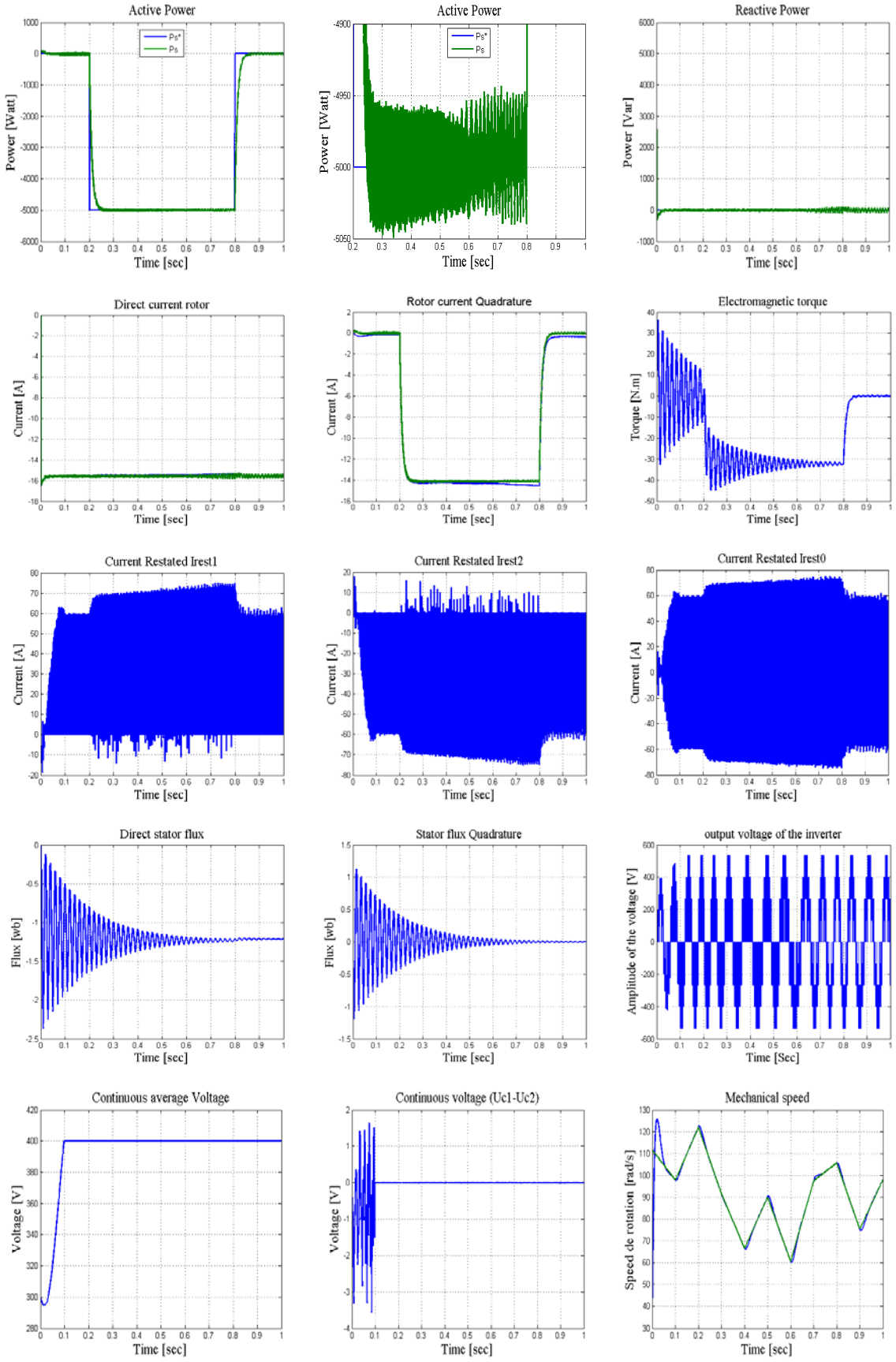

Figure10. Behavior of the powers of DFIG with indirect vector control with loop power controlled by FSMC.

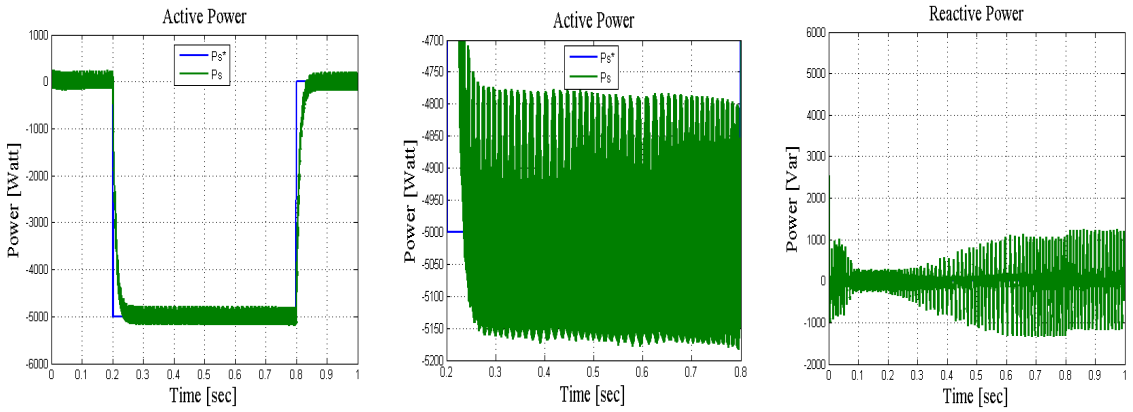

Figure 11. Behavior of the powers of DFIG with indirect vector control with loop power controlled by SMC.

The simulation results show different curves are obtained by controlling the active and reactive power generated at the stator of the DFIG. This control technique allows you to decouple the expressions of active and reactive power of the generator or in the flux and torque.

According to the results, we find that the indirect control with loop power controller using SMC or FSMC have good decoupling control of active and reactive power at the stator. After a transitional regime the differente paramaters persute perfectly their reference.

The reactive power is zero and it is a condition of operation of the DFIG for a unity power factor. As we reported earlier that the disadvantage of the SMC is the riples. To reduce it, we combined this control with fuzzy logic to build a new structure called FSMC, which allows reducing the chattering phenomena of over 75% in our study.

We can see that the stator flux follows the following reference axis (d) with almost zero quadrature components, which means that the decoupling of the machine is successful. It is clear that the quadrature component of the rotor current Irq control the electromagnetic torque so the active power. The direct component of the rotor current, and thus control the flow of reactive power transmitted between the stator and the network. This is found in the changes in direct and quadrature components of rotor currents, which are the images of active and reactive powers. Note that the electromagnetic torque reacts spontaneously when there is a demand for active power, reactive power independently

We observe that the current Irest1 presents a look opposite to that of Irest2. This is necessary for the current Irest0 has a zero mean value. As can be seen, the current Irest0 is substantially zero mean value. Note that the two DC voltages well below their reference and we also find that the difference between the two voltages is practically zero after a transient 0.1s which mean a better stability of the midpoint

In this section, it is explained the results of research and at the same time is given the comprehensive discussion. Results can be presented in figures, graphs, tables and others that make the reader understand easily [2], [5]. The discussion can be made in several sub-chapters.

4. CONCLUSION

This work has allowed us to study the modeling of a chain of wind conversion based on DFIG consists of a rectifier control by the PWM technique, and a DC bus, all connected to the network via a PWM inverter and a filter.

We studied the indirect vector control loop power DFIG which allows a decoupling between the flux and torque.

The control is provided by two orders SMC and FSMC for which we found the performance of the latter relative to the SMC perspective chattering.

Provide a statement that what is expected, as stated in the "Introduction" chapter can ultimately result in "Results and Discussion" chapter, so there is compatibility. Moreover, it can also be added the prospect of the development of research results and application prospects of further studies into the next (based on result and discussion).

REFERENCES

[1] M. Adjoudj et al, "Sliding mode control of a doubly fed induction generator for wind turbines", conversion systems. Rev. Roum. Sci. Techn. – Électrotechn. et Énerg., 56, 1, pp. 15-24, 2011.
[2] Slotine, J.J.E. Li, "Applied nonlinear control", Prence Hall, USA, 1998.
[3] Reema Manavalan, C Senthil Kumar, "Analysis of Hybrid Renewable Energy System using NPC Inverter", Research Inventy: International Journal Of Engineering And Science Issn: 2278-4721, Vol.2, Issue 7 (March 2013), Pp 26-30.
[4] G. Abad J. Lopez, M.A. Rodrıguez, L. Marroyo, G. Iwanski, "Doubly fed induction machine: modeling and control for wind energy generation", IEEE press Series on Power Engineering, aug 2011.
[5] Mohamed Hilal,Youssef Errami, Mohamed Benchagra And Mohamed Maaroufi "Fuzzy Power Control For Doubly Fed Induction Generator Based Wind Farm," Journal of Theoretical and Applied Information Technology 30th September 2012. Vol. 43 No.2.
[6] F. Valenciaga C.A. Evangelista "Sliding active and reactive power control of a wind energy conversion system". Published in IET Control Theory and Applications. Received on 26th August 2009. Revised on 25th December 2009. Doi: 10.1049/iet-cta.2009.0437
[7] F. Kendouli, K. Nabti, K. Labed and H. Benalla, "Modeling, simulation and control of a variable speed wind turbine based on doubly-fed induction generator." Journal of Renewable Energy Vol. 14 No. 1 (2011) 109-120.
[8] B.Belabbas, "Control by PI Fuwwy energy DFIG and a variable speed turbine (MPPT)." International Conference on Renewable Energies Bejaia (2012).
[9] Souhila Benmansour Aboura, "Hybrid fuzzy sliding control method applied to a robot manipulator dynamic hyper "
[10] Abdelfettah kerboua; Mohamed abid, "hybrid fuzzy sliding mode control of a doubly-fed induction generator in wind turbines." Automatic and computers.
[11] Y. Mishra, S. Mishra, Li. Fangxing, Zhao Yang Dong, R.C. Bansal, "Small-Signal Stability Analysis of a DFIG-Based Wind Power System Under Different Modes of Operation", IEEE Transactions on Energy Conversion, Vol. 24, pp. 972 –982, Dec. 2009.
[12] M. Mohseni, S. Islam, "An improved modeling and control approach for DFIG-based wind generation systems", Power Engineering Conference, 2009. AUPEC 2009. Australasian Universities, 27-30, pp. 1–6, Sept. 2009.
[13] J.B. Ekanayake, L. Holdsworth, X. Wu and N. Jenkins, "Dynamic Modeling of Doubly Fed Induction Generator Wind Turbine", IEEE Transactions on Power Systems, Vol. 18, N°. 2, pp. 803–809, May. 2003.
[14] Lie Xu and Philip Cartwright, "Direct Active and Reactive Power Control of DFIG for Wind Energy Generator", IEEE Transactions on Energy Conversion, Vol. 21, N°. 3, pp. 750–758, September. 2006.